Liquid-induced damping of mechanical feedback effects in single electron tunneling through a suspended carbon nanotube

D. R. Schmid,[1] P. L. Stiller,[1] Ch. Strunk,[1] and A. K. Hüttel[1, a)]
Institute for Experimental and Applied Physics, University of Regensburg, Universitätsstr. 31, 93053 Regensburg, Germany

(Dated: 24 September 2015)

In single electron tunneling through clean, suspended carbon nanotube devices at low temperature, distinct switching phenomena have regularly been observed. These can be explained via strong interaction of single electron tunneling and vibrational motion of the nanotube. We present measurements on a highly stable nanotube device, subsequently recorded in the vacuum chamber of a dilution refrigerator and immersed in the ^{3}He/^{4}He mixture of a second dilution refrigerator. The switching phenomena are absent when the sample is kept in the viscous liquid, additionally supporting the interpretation of dc-driven vibration. Transport measurements in liquid helium can thus be used for finite bias spectroscopy where otherwise the mechanical effects would dominate the current.

(c) AIP Publishing LLC http://dx.doi.org/10.1063/1.4931775

arXiv:1407.2114v3 [cond-mat.mes-hall] 23 Sep 2015

Clean, suspended carbon nanotubes provide an extremely versatile model system. As nano-electromechanical beam resonators, they can be tuned over a large tension and thereby also frequency range.[1–5] At cryogenic temperatures, very high mechanical quality factors have been observed,[3,6,7] making the observation of non-trivial interaction between single electron charging and the mechanical motion possible.[8–11] Both electronic tunneling[10,12] and magnetic induction[13,14] have been shown to induce damping and thereby reduce the effective mechanical quality factor.

In addition, clean carbon nanotubes also provide highly regular transport spectra, making the analysis of single[15] and multi quantum dot systems[16] possible. An unexpected feature in dc measurements was the observation of regions with suppressed or enhanced current level and abrupt, switching-like edges.[8,13] These switching phenomena limit the ability to do finite bias spectroscopy at transparent tunnel barriers. They are consistent with feedback effects due to strong coupling between single electron tunneling and mechanical motion, as detailed in Ref. 17. The positive feedback between electronic tunneling and mechanical motion gives rise to self-oscillation of the vibration mode and in turn leads to an abrupt change in the current through and in the conductance of the quantum dot embedded on the mechanically active part of the carbon nanotube.

In this manuscript we compare measurements on a highly stable carbon nanotube quantum dot device, which was subsequently cooled down first in the vacuum chamber of a conventional dilution refrigerator and afterwards within the ^{3}He/^{4}He mixture (dilute phase) of a top-loading dilution refrigerator. A distinct difference between the measurement runs is that the abovementioned switching phenomena are absent when the sample is immersed into the viscous liquid ^{3}He/^{4}He mixture. This provides additional support for their vibrational origin.

Our device consists of a clean carbon nanotube grown via chemical vapor deposition across a pre-fabricated trench and rhenium electrodes. Fabrication and structure details can be found in previous publications, as well as additional measurement data on the same device.[13,18] Electronic transport measurements were performed subsequently in two dilution refrigerators at $25\,\mathrm{mK} \lesssim T_{\mathrm{MC,base}} \lesssim 30\,\mathrm{mK}$. During the first of these cooldowns, the device was in vacuum environment, in the second cooldown using a top-loading dilution refrigerator the sample was mounted within the liquid ^{3}He/^{4}He mixture (dilute phase) of the mixing chamber.

The inset of Fig. 1 shows a simplified sketch of the electronic measurement setup, as typically used in Coulomb blockade spectroscopy:[19] a gate voltage V_g and a bias voltage V_sd are applied, and the resulting current is converted to a voltage at room temperature and recorded. As can be seen from conductance measurements as in Fig. 1(a) and Fig. 1(b), a small band gap separates the highly transparent hole conduction side (not shown here) from sharp Coulomb blockade oscillations in electron conduction. At higher electron number N_el the tunnel barriers to the contacts become increasingly transparent, and co-tunneling and regular Kondo enhancement of the conductance emerge.[18,20]

Fig. 1(a) and Fig. 1(b) compare the low-bias conductance of the device in the two subsequent cooldowns in vacuum (Fig. 1(a)) and ^{3}He/^{4}He mixture (Fig. 1(b)); a highly regular addition spectrum emerges in both cases. By recording current at increasingly large bias voltages and long amplifier integration times, as e.g. plotted in Fig. 1(c), the first Coulomb oscillation next to the electronic band gap has been identified in both cases, providing the absolute number of trapped electrons. In liquid environment, the Coulomb blockade oscillations are shifted towards lower gate voltage; the gate voltage position of the Nth conductance maximum approximately follows a linear scaling $V_\mathrm{g}^\mathrm{vac}(N) \approx 1.037 \times V_\mathrm{g}^\mathrm{LHe}(N) - 0.01\,\mathrm{V}$,

a)Electronic mail: andreas.huettel@ur.de

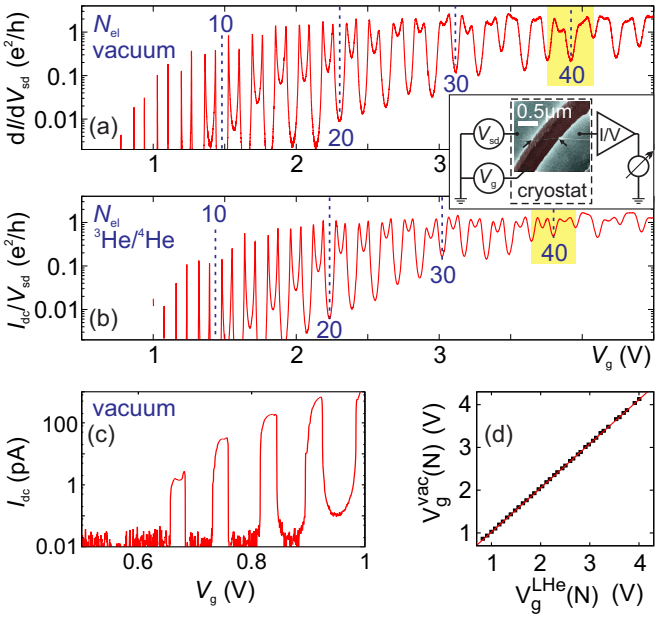

FIG. 1. (Color online) (a) Low-bias differential conductance $\mathrm{d}I/\mathrm{d}V_{\mathrm{sd}}$ of a carbon nanotube as a function of the gate voltage V_{g}, at dilution refrigerator base temperature in vacuum (lock-in measurement using $V_{\mathrm{sd,ac}} = 5\,\mu\mathrm{V}$ at $f_{\mathrm{sd}} = 137.7\,\mathrm{Hz}$). A Coulomb blockade dominated few electron regime is visible. For higher electron numbers N_{el} the tunnel rates gradually increase. Inset: Scanning electron micrograph of a similar carbon nanotube device with a simplified schematic of the measurement setup. (b) Conductance from a dc measurement $I_{\mathrm{dc}}(V_{\mathrm{g}})$ at $V_{\mathrm{sd,dc}} = 105\,\mu\mathrm{V}$, subsequent cooldown in ^{3}He/^{4}He mixture. In both cases, the gate voltage range shown in Fig. 3 is shaded yellow. (c) Example measurement of the dc current at high bias $V_{\mathrm{sd}} = 12\,\mathrm{mV}$, displaying the first Coulomb oscillations next to the nanotube band gap (vacuum case). (d) Single electron tunneling peak positions from (a) and (b). For each data point, the x-coordinate is given by the peak gate voltage in Helium (from (b)) and the y-coordinate by the corresponding peak gate voltage in vacuum (from (a)).

see also Fig. 1(d). Such a scaling is already expected from the much-simplified model of a classical single electron transistor, see e.g. Ref. 19, where the distance between Coulomb oscillations ΔV_{g} is given by $\Delta V_{\mathrm{g}} = e/C_g$. In our device, only part of the volume between nanotube and highly doped gate substrate is etched and thereby changes dielectric constant between cooldowns. Thus, the scaling of the gate capacitance C_g is consistent with the upper bound given by the liquid helium dielectric constant[21] $\epsilon_{r,^4\mathrm{He}} \approx 1.06$.

In vacuum environment measurements, following Ref. 3, the device displays under rf irradiation a clear resonant gate-dependent signal which can be attributed to the transversal vibration mode. This is illustrated in Fig. 2(a) and Fig. 2(b), displaying a large scale measurement[3] as well as an exemplary detail zoom into one Coulomb blockade oscillation.[8] Mechanical quality factors of $Q \simeq 25000$ have been observed; see Ref. 13 for a discussion of driven vibrations and the magnetic field

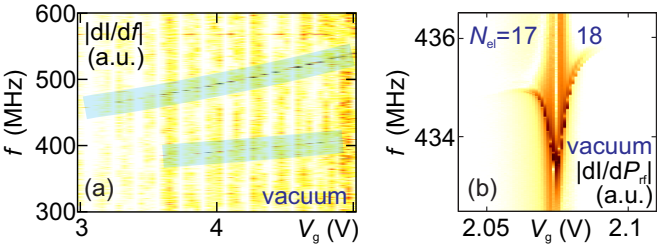

FIG. 2. (Color online) (a) dc-detection of transversal mechanical resonances under contact-free rf irradiation, following Refs. 3 and 4: $|\mathrm{d}I_{\mathrm{dc}}/\mathrm{d}f|$ as function of gate voltage V_{g} and driving frequency f; two gate-dependent mechanical resonances are highlighted. (b) Exemplary detection of a mechanical resonance across one Coulomb oscillation, cf. Refs. 4, 8, and 10. The rf source power is slowly modulated and the corresponding variation in current detected.

dependence of mechanical effects.

In the following we focus on the intermediate coupling regime around $N_{\mathrm{el}} = 40$, shaded (yellow) in Fig. 1(a,b), where the Kondo effect dominates the low-bias conductance in the Coulomb valleys with odd electron numbers. For a closer investigation the current is measured as function of gate voltage V_{g} and bias voltage V_{sd}, yielding the quantum dot stability diagram. The clean and essentially unchanged electronic structure allows us to compare measurements from two cool-downs but for the same quantum dot parameter regime.

Figure 3 contrasts those measurements and again demonstrates the consistency of the electronic features. The wide high conductance ridges at odd electon number N_{el} are a manifestation of the Kondo effect;[18,20,22] its strong emergence at odd electron numbers is already clearly visible in Fig. 1(a,b) for $N > 10$. The overall reduced conductance closely around $V_{\mathrm{sd}} = 0$ accompanied by two lines of enhanced conductance at low finite V_{sd} can be tentatively attributed to the presence of an energy gap Δ in the superconducting rhenium contacts[23,24] and is also similar in both measurements. At a finite voltage of $eV_{\mathrm{sd}} = \pm 2\Delta$ the onset of quasiparticle cotunneling leads to additional conductance.

While in Fig. 3(a) the sample is in vacuum, in (b) the sample is immersed into liquid ^{3}He/^{4}He mixture (diluted phase). A significant difference between the two data sets is given by the sharp spikes in the conductance in vacuum, Fig. 3(a), highlighted with white arrows, framing regions of enhanced or suppressed current level. This phenomenon is well understood by a positive feedback between single electron tunneling and the mechanical motion.[17] It requires large tunnel rates between quantum dot and leads; first traces of the effect are already visible at much lower electron number (see also Ref. 18 Fig. 11). In the measurement of Fig. 3(b), plotted at identical y-axis scaling, these feedback-induced phenomena are clearly absent, even up to a much higher bias voltage.[25]

While electronic damping mechanisms have been

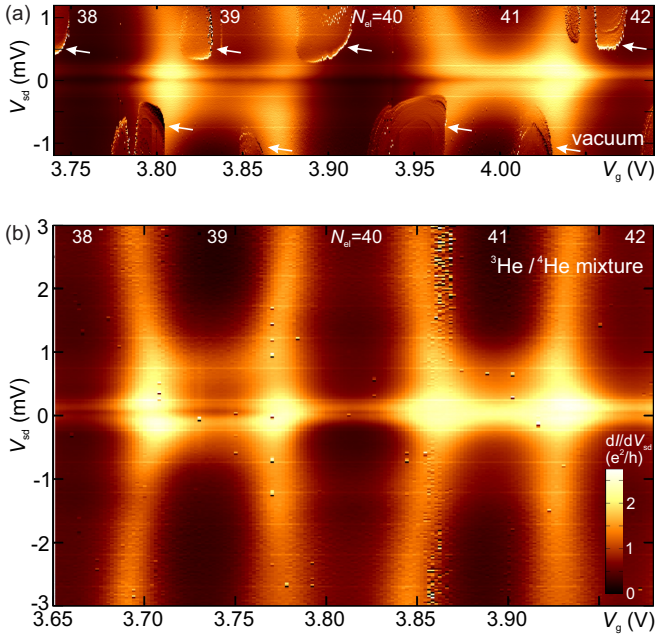

FIG. 3. (Color online) (a) Numerically derived differential conductance $\mathrm{d}I/\mathrm{d}V_{\mathrm{sd}}$ as function of bias voltage V_{sd} and gate voltage V_{g}. The device is in vacuum. Kondo ridges of enhanced conductance[18,20,22] are clearly visible; the dark line of lower conductance at $V_{\mathrm{sd}} = 0$ reflects the superconducting energy gap of the rhenium contacts. At finite bias, distinct switching phenomena due to electromechanical feedback[8,13,17] are clearly visible (white arrows). Related data has already been published in Ref. 13, Figure 2. (b) Comparable measurement of the same sample, but now immersed into the liquid ^{3}He/^{4}He mixture of a dilution refrigerator; same V_{sd} scaling. The switching phenomena are clearly absent even for significantly higher bias voltage V_{sd}.

demonstrated recently,[10,13] here the viscous ^{3}He/^{4}He fluid surrounding the carbon nanotube adds purely mechanical damping, reduces the high quality factor of the mechanical system, and suppresses self-oscillation in the system. This provides a much more direct confirmation that mechanical motion is the underlying mechanism for the switching phenomena.

Mechanical resonators have long been used for viscosity measurements in low-temperature physics, and recently also nanomechanical systems have entered this field.[26–28] The unusual parameter combination present in our setup, combining a ^{3}He/^{4}He fluid at millikelvin temperatures with a beam diameter on the order $\sim 1\,\mathrm{nm}$ and resonance frequencies $\sim 250\,\mathrm{MHz}$,[13] poses however challenges for a detailed estimate on the damping mechanisms. The viscosity of the diluted phase of a ^{3}He/^{4}He mixture at $T \simeq 25\,\mathrm{mK}$ is $\eta \sim 10^{-4}\,\mathrm{N\,s/m^2}$.[21] This is roughly an order of magnitude larger than the viscosity of air at room temperature and standard condition in pressure, $\eta \sim 10^{-5}\,\mathrm{N\,s/m^2}$. Since at room temperature already a much smaller gas pressure of $p \sim 1000\,\mathrm{Pa}$ causes a reduction of the effective mechanical quality factor of carbon nanotube resonators to $Q \ll 100$,[1,29] a strong mechanical damping by the viscous medium is expected.

Apart from damping of the vibrational mode, in addition, the ^{3}He/^{4}He liquid naturally leads to improved thermalization of the entire chip structure and the cables connecting to it. However, the transversal vibration quality factor of a carbon nanotube device increases at lower temperature[3] – which, as dominant effect, would enhance switching effects rather than suppressing them.[8,13,17]

In conclusion, we give an intuitive demonstration of the mechanical origin of switching phenomena[8,13,17] observed in freely suspended carbon nanotubes by comparison of measurements in different sample environments. Keeping the electronic properties almost unaffected, a viscous ^{3}He/^{4}He medium supplies an additional damping mechanism and prevents feedback-induced oscillation. Hence, this damping mechanism provides a way to circumvent instabilities in finite bias spectroscopy on overgrown freely suspended carbon nanotubes without restriction of the accessible temperature, magnetic field, and tunnel coupling range.

ACKNOWLEDGMENTS

The authors acknowledge financial support by the Deutsche Forschungsgemeinschaft (Emmy Noether grant Hu 1808/1, GRK 1570, SFB 631 TP A11) and by the Studienstiftung des deutschen Volkes. We thank A. Dirnaichner for experimental support.

[1] V. Sazonova, Y. Yaish, H. Üstünel, D. Roundy, T. A. Arias, and P. L. McEuen, "A tunable carbon nanotube electromechanical oscillator," Nature **431**, 284 (2004).
[2] B. Witkamp, M. Poot, and H. S. J. van der Zant, "Bending-mode vibration of a suspended nanotube resonator," Nano Letters **6**, 2904 (2006).
[3] A. K. Hüttel, G. A. Steele, B. Witkamp, M. Poot, L. P. Kouwenhoven, and H. S. J. van der Zant, "Carbon nanotubes as ultrahigh quality factor mechanical resonators," Nano Letters **9**, 2547–2552 (2009).
[4] A. K. Hüttel, H. B. Meerwaldt, G. A. Steele, M. Poot, B. Witkamp, L. P. Kouwenhoven, and H. S. J. van der Zant, "Single electron tunnelling through high-Q single-wall carbon nanotube NEMS resonators," physica status solidi (b) **247**, 2974 (2010).
[5] P. L. Stiller, S. Kugler, D. R. Schmid, C. Strunk, and A. K. Hüttel, "Negative frequency tuning of a carbon nanotube nanoelectromechanical resonator under tension," physica status solidi (b) **250**, 2518–2522 (2013).
[6] J. O. Island, V. Tayari, A. C. McRae, and A. R. Champagne, "Few-Hundred GHz carbon nanotube nanoelectromechanical systems (NEMS)," Nano Letters **12**, 4564–4569 (2012).
[7] J. Moser, A. Eichler, J. Güttinger, M. I. Dykman, and A. Bachtold, "Nanotube mechanical resonators with quality factors of up to 5 million," Nature Nanotechnology **9**, 1007–1011 (2014).
[8] G. A. Steele, A. K. Hüttel, B. Witkamp, M. Poot, H. B. Meerwaldt, L. P. Kouwenhoven, and H. S. J. van der Zant, "Strong Coupling Between Single-Electron Tunneling and Nanomechanical Motion," Science **325**, 1103–1107 (2009).
[9] B. Lassagne, Y. Tarakanov, J. Kinaret, D. Garcia-Sanchez, and A. Bachtold, "Coupling mechanics to charge transport in carbon nanotube mechanical resonators," Science **28**, 1107 (2009).

[10]H. B. Meerwaldt, G. Labadze, B. H. Schneider, A. Taspinar, Y. M. Blanter, H. S. J. van der Zant, and G. A. Steele, "Probing the charge of a quantum dot with a nanomechanical resonator," Physical Review B **86**, 115454 (2012).
[11]A. Benyamini, A. Hamo, S. V. Kusminskiy, F. von Oppen, and S. Ilani, "Real-space tailoring of the electron-phonon coupling in ultraclean nanotube mechanical resonators," Nature Physics **10**, 151–156 (2014).
[12]M. Ganzhorn and W. Wernsdorfer, "Dynamics and dissipation induced by single-electron tunneling in carbon nanotube nanoelectromechanical systems," Physical Review Letters **108**, 175502 (2012).
[13]D. R. Schmid, P. L. Stiller, C. Strunk, and A. K. Hüttel, "Magnetic damping of a carbon nanotube nano-electromechanical resonator," New Journal of Physics **14**, 083024 (2012).
[14]A. Nocera, C. A. Perroni, V. M. Ramaglia, G. Cantele, and V. Cataudella, "Magnetic effects on nonlinear mechanical properties of a suspended carbon nanotube," Physical Review B **87**, 155435 (2013).
[15]J. Cao, Q. Wang, and H. Dai, "Electron transport in very clean, as-grown suspended carbon nanotubes," Nature Materials **4**, 745–749 (2005).
[16]G. A. Steele, G. Götz, and L. P. Kouwenhoven, "Tunable few-electron double quantum dots and Klein tunnelling in ultraclean carbon nanotubes," Nature Nanotechnology **4**, 363–367 (2009).
[17]O. Usmani, Y. M. Blanter, and Y. Nazarov, "Strong feedback and current noise in nanoelectromechanical systems," Physical Review B **75**, 195312 (2007).
[18]D. R. Schmid, S. Smirnov, M. Margańska, A. Dirnaichner, P. L. Stiller, M. Grifoni, A. K. Hüttel, and C. Strunk, "Broken SU(4) symmetry in a Kondo-correlated carbon nanotube," Physical Review B **91**, 155435 (2015).
[19]L. P. Kouwenhoven, C. M. Marcus, P. L. McEuen, S. Tarucha, R. M. Westervelt, and N. S. Wingreen, "Electron transport in quantum dots," in *Mesoscopic Electron Transport*, edited by L. L. Sohn, L. P. Kouwenhoven, and G. Schön (Kluwer, 1997).
[20]D. Goldhaber-Gordon, H. Shtrikman, D. Mahalu, D. Abusch-Magder, U. Meirav, and M. A. Kastner, "Kondo effect in a single-electron transistor," Nature **391**, 156–159 (1998).
[21]C. Enss and S. Hunklinger, *Low-Temperature Physics* (Springer-Verlag, 2005).
[22]J. Nygård, H. C. Cobden, and P. E. Lindelof, "Kondo physics in carbon nanotubes," Nature **408**, 342 (2000).
[23]K. Grove-Rasmussen, H. I. Jørgensen, B. M. Andersen, J. Paaske, T. S. Jespersen, J. Nygård, K. Flensberg, and P. E. Lindelof, "Superconductivity-enhanced bias spectroscopy in carbon nanotube quantum dots," Phys. Rev. B **79**, 134518 (2009).
[24]S. Ratz, A. Donarini, D. Steininger, T. Geiger, A. Kumar, A. K. Hüttel, C. Strunk, and M. Grifoni, "Thermally induced subgap features in the cotunneling spectroscopy of a carbon nanotube," New Journal of Physics **16**, 123040 (2014).
[25] A distinct fluctuation is visible in Fig. 3(b) at $V_\mathrm{g} = 3.86\,\mathrm{V}$. Similar phenomena occur at $V_\mathrm{g} = 3.44\,\mathrm{V}$ and $V_\mathrm{g} = 4.25\,\mathrm{V}$. They display only very weak dependence on bias voltage over the measured range $-8\,\mathrm{mV} \leq V_\mathrm{sd} \leq 8\,\mathrm{mV}$, and their gate voltage position does not stand in any clear relation to the position of the Coluomb blockade oscillations. Both these observations indicate that a charge trap unrelated but close to the quantum dot at hand is triggered.
[26]A. Kraus, A. Erbe, and R. H. Blick, "Nanomechanical vibrating wire resonator for phonon spectroscopy in liquid helium," Nanotechnology **11**, 165 (2000).
[27]E. Collin, T. Moutonet, J.-S. Heron, O. Bourgeois, Y. Bunkov, and H. Godfrin, "A tunable hybrid electro-magnetomotive NEMS device for low temperature physics," Journal of Low Temperature Physics **162**, 653–660 (2011).
[28]M. González, P. Zheng, E. Garcell, Y. Lee, and H. B. Chan, "Comb-drive micro-electro-mechanical systems oscillators for low temperature experiments," Review of Scientific Instruments **84**, 025003 (2013).
[29]S. Fukami, T. Arie, and S. Akita, "Effect of gaseous dissipation of oscillating cantilevered carbon nanotubes," Japanese Journal of Applied Physics **48**, 06FG04 (2009).